PHYSICAL REVIEW D **90,** 065033 (2014)

N_{eff} in low-scale seesaw models versus the lightest neutrino mass

P. Hernández,[1,*] M. Kekic,[1,†] and J. Lopez-Pavon[2,3,‡]

[1]*IFIC (CSIC) and Departamento Física Teórica, Universidad de Valencia, Edificio Institutos Investigación, Apartado de Correos 22085, E-46071 Valencia, Spain*

[2]*SISSA, via Bonomea 265, 34136 Trieste, Italy*

[3]*INFN, sezione di Trieste, 34136 Trieste, Italy*

(Received 19 June 2014; published 25 September 2014)

We evaluate the contribution to N_{eff} of the extra sterile states in low-scale type I seesaw models (with three extra sterile states). We explore the full parameter space and find that at least two of the heavy states always reach thermalization in the early Universe, while the third one might not thermalize provided the lightest neutrino mass is below $\mathcal{O}(10^{-3}\text{ eV})$. Constraints from cosmology therefore severely restrict the spectra of heavy states in the range 1 eV–100 MeV. The implications for neutrinoless double beta decay are also discussed.

DOI: 10.1103/PhysRevD.90.065033 PACS numbers: 14.60.St, 98.80.Cq

I. INTRODUCTION

The simplest extension of the standard model (SM) that can account for the observed neutrino masses is a type I seesaw model [1] with $N \geq 2$ extra singlet Majorana fermions. The Majorana masses, that we globally denote as M, constitute a new scale of physics (the seesaw scale) which is presently unknown. Since the light neutrino masses are a combination of the Yukawa couplings, the electroweak scale and the seesaw scale, the latter can be arbitrary if the Yukawas are adjusted accordingly. As a result, the seesaw scale is presently unconstrained to lie anywhere above $\mathcal{O}(\text{eV})$ up to $\mathcal{O}(10^{15}\text{ GeV})$ [2]. The determination of this scale is one of the most important open questions in neutrino physics.

It is often assumed that the seesaw scale is very high, above the electroweak scale. However, in the absence of any other hint of new physics beyond the SM, the possibility that the seesaw scale could be at the electroweak scale or lower should be seriously considered. As far as naturalness goes, the model with a low scale is technically natural, since in the limit $M \to 0$, a global lepton number symmetry is recovered: neutrinos becoming Dirac particles by the pairing of the Majorana fermions.

The spectra of $N = 3$ type I seesaw models contain six Majorana neutrinos: the three lightest neutrinos, mostly active, and three heavier, mostly sterile. The coupling of the latter with the leptons, U_{as}, is strongly correlated with their masses (the naive seesaw scaling being $|U_{as}|^2 \propto M^{-1}$). The possibility that such neutrino sterile states could be responsible for any of the anomalies found in various experiments is of course very interesting, since it could open a new window into establishing the new physics of neutrino masses.

Models with extra light sterile neutrinos with masses in the range of $\mathcal{O}(\text{eV})$ could provide an explanation to the LSND/MiniBOONE [5,6] and reactor anomalies [7]. Sterile species in the $\mathcal{O}(\text{keV})$ range could still be valid candidates for warm dark matter [8–11]. The recent measurement of an x-ray signal [12,13] might be the first experimental indication of such possibility. Species in the $\mathcal{O}(\text{GeV})$ range could account for the baryon asymmetry in the Universe [14,15] (for a recent review see [16]).

There are important constraints on low-scale models from direct searches and rare processes such as $\mu \to e\gamma$ and μe conversion. Recent results can be found in [17–19]. The constraints are strongly dependent on M for $M \lesssim \mathcal{O}(100\text{ GeV})$.

It is well known that if light sterile neutrinos with significant active-sterile mixing exist they can contribute significantly to the energy density of the Universe. Mechanisms to reduce this contribution have been proposed, such as the presence of primordial lepton asymmetries [20] or new interactions [21,22], which however typically require new physics beyond that of the sterile species. The energy density of the extra neutrino species, ϵ_s, is usually quantified in terms of ΔN_{eff} (when they are relativistic) defined by

$$\Delta N_{\text{eff}} \equiv \frac{\epsilon_s}{\epsilon_\nu^0}, \tag{1}$$

where ϵ_ν^0 is the energy density of one SM massless neutrino with a thermal distribution [below $e^\pm$ annihilation it is $\epsilon_\nu^0 \equiv (7\pi^2/120)(4/11)^{4/3}T_\gamma^4$ at the photon temperature T_γ]. One fully thermal extra sterile state that decouples from the thermal bath being relativistic contributes $\Delta N_{\text{eff}} \simeq 1$ when it decouples.

N_{eff} at big bang nucleosynthesis (BBN) strongly influences the primordial helium production. A recent analysis of BBN bounds [23] gives $N_{\text{eff}}^{\text{BBN}} = 3.5 \pm 0.2$.

*m.pilar.hernandez@uv.es
†Marija.Kekic@ific.uv.es
‡jlpavon@sissa.it

$N_{\rm eff}$ also affects the anisotropies of the cosmic microwave background (CMB). Recent CMB measurements from Planck give $N_{\rm eff}^{\rm CMB} = 3.30 \pm 0.27$ [24], which includes WMAP-9 polarization data [25] and high multipole measurements from the South Pole Telescope [26] and the Atacama Cosmology Telescope [27]. Recent global analyses, including the BICEP2 results [28,29], seem to prefer larger values of $N_{\rm eff}^{\rm CMB}$ [30–32].

The contribution of extra sterile neutrinos to $N_{\rm eff}$ has been extensively studied in phenomenological models, where there is no correlation between masses and mixing angles [33–35]. For recent analyses of eV scale neutrinos, with and without lepton asymmetries, see [36–42]. In [43] we explored systematically the contribution to $N_{\rm eff}$ of the minimal type I seesaw models with just two extra singlets, $N = 2$. We found that whenever the two heavier states are below $\mathcal{O}(100~\text{MeV})$, they contribute too much energy/matter density to the Universe, while the possibility of having one state $\lesssim$ eV and another heavier than 100 MeV may not be excluded by cosmological and oscillation data constraints, but requires further scrutiny.

The purpose of this paper is to perform the same study in the next-to-minimal seesaw model where $N = 3$. This is the standard type I seesaw model with a low scale, and is also often referred to as the neutrino Minimal Standard Model (νMSM). This model has been extensively studied in the literature, concentrating on regions of parameter space where the lightest sterile state could be a warm dark matter particle, and the two heavier states could be responsible for the baryon asymmetry in the Universe [15]. What we add in this paper is a systematic study of the full parameter space to understand the constraints on the seesaw scale(s) from the modifications to the standard cosmology induced by the three heavy neutrino states. We will assume that primordial lepton asymmetries are negligible. Although the model in principle satisfies the Sakharov conditions to generate a lepton asymmetry, previous works indicate that significant lepton asymmetries can only be generated when at least two of the sterile states are heavy enough, $\mathcal{O}(\text{GeV})$, and extremely degenerate [44]. Here we will concentrate on studying the bounds from cosmology when such an extreme degeneracy of the sterile neutrino states is not present. We show that, in spite of the large parameter space, the thermalization of the sterile states in this model is essentially controlled by one parameter: the lightest neutrino mass.

The paper is organized as follows. In Sec. II we review the estimates of the thermalization rate of the sterile states as derived in [43], which allow us to efficiently explore the full parameter space of the model. In Sec. III we derive analytical bounds for the thermalization rate and in Sec. IV we correlate $\Delta N_{\rm eff}$ with the lightest neutrino mass. In Sec. V we present numerical results from solving the Boltzmann equations and finally in Sec. VI we analyze the impact on neutrinoless double beta decay. In Sec. VII we conclude.

II. THERMALIZATION OF STERILE NEUTRINOS IN 3 + 3 SEESAW MODELS

The model is described by the most general renormalizable Lagrangian including $N = 3$ extra singlet Weyl fermions, ν_R^i:

$$\mathcal{L} = \mathcal{L}_{\rm SM} - \sum_{\alpha,i} \bar{L}^\alpha Y^{\alpha i} \tilde{\Phi} \nu_R^i - \sum_{i,j=1}^{3} \frac{1}{2} \bar{\nu}_R^{ic} M_N^{ij} \nu_R^j + \text{H.c.},$$

where Y is a 3×3 complex matrix and M_N a diagonal real matrix. The spectrum of this theory has six massive Majorana neutrinos, and the mixing is described in terms of six angles and six charge parity (CP) phases.

We assume that the eigenvalues of M_N are significantly larger than the atmospheric and solar neutrino mass splittings, which implies a hierarchy $M_N \gg Yv$ and therefore the seesaw approximation is good. A convenient parametrization in this case is provided by that of Casas-Ibarra [45], or its extension to all orders in the seesaw expansion as described in [46] (for an alternative see [47]). The mass matrix can be written as

$$\mathcal{M}_\nu = U^* \text{Diag}(m_l, M_h) U^\dagger, \tag{2}$$

where $m_l = \text{Diag}(m_1, m_2, m_3)$ and $M_h = \text{Diag}(M_1, M_2, M_3)$. Denoting by a the active/light neutrinos and s the sterile/heavy species, the unitary matrix can be written as

$$U = \begin{pmatrix} U_{aa} & U_{as} \\ U_{sa} & U_{ss} \end{pmatrix}, \tag{3}$$

with

$$\begin{aligned} U_{aa} &= U_{\rm PMNS} \mathcal{H}, \\ U_{ss} &= \bar{\mathcal{H}}, \\ U_{sa} &= i \bar{\mathcal{H}} M_h^{-1/2} R m_l^{1/2}, \\ U_{as} &= i U_{\rm PMNS} \mathcal{H} m_l^{1/2} R^\dagger M_h^{-1/2}, \end{aligned} \tag{4}$$

where $U_{\rm PMNS}$ is a 3×3 unitary matrix and R is a generic 3×3 orthogonal complex matrix, while $\mathcal{H}$ and $\bar{\mathcal{H}}$ are defined by

$$\begin{aligned} \mathcal{H}^{-2} &= I + m_l^{1/2} R^\dagger M_h^{-1} R m_l^{1/2}, \\ \bar{\mathcal{H}}^{-2} &= I + M_h^{-1/2} R m_l R^\dagger M_h^{-1/2}. \end{aligned} \tag{5}$$

At leading order in the seesaw expansion, i.e. up to $\mathcal{O}(\frac{m_l}{M_h})$, $\mathcal{H} \simeq \bar{\mathcal{H}} \simeq 1$, and we recover the Casas-Ibarra parametrization. In this approximation $U_{\rm PMNS}$ is the light neutrino mixing matrix measured in oscillations.

Neutrino oscillation data fix two of the three eigenvalues in m_l and the three angles in $U_{\rm PMNS}$; however all the heavy masses in M_h, the lightest neutrino mass in m_l, the three complex angles in R and the three CP violating phases in $U_{\rm PMNS}$ are presently unconstrained [48].

In [49] a simple estimate for the thermalization of one sterile neutrino in the early Universe, neglecting primordial lepton asymmetries, was given as follows. Assuming that the active neutrinos are in thermal equilibrium with a collision rate given by Γ_{ν_α}, the collision rate for the sterile neutrinos can be estimated to be

$$\Gamma_{s_j} \simeq \frac{1}{2}\sum_a \langle P(\nu_a \to \nu_{s_j})\rangle \times \Gamma_{\nu_\alpha}, \tag{6}$$

where $\langle P(\nu_\alpha \to \nu_{s_j})\rangle$ is the time-averaged probability $\nu_\alpha \to \nu_{s_j}$. This probability depends strongly on temperature because the neutrino index of refraction in the early Universe is modified by coherent scattering of neutrinos with the particles in the plasma [50]. Thermalization will be achieved if there is any temperature where this rate is higher than the Hubble expansion rate, i.e. $\Gamma_{s_j}(T) \geq H(T)$. In a radiation-dominated universe, $H(T) = \sqrt{\frac{4\pi^3 g_*(T)}{45}}\frac{T^2}{M_{\rm Planck}}$, with $g_*(T)$ being the number of relativistic degrees of freedom.

One can therefore define the function $f_{s_j}(T)$, which measures the sterile production rate of the species s_j in units of the Hubble expansion rate,

$$f_{s_j}(T) \equiv \frac{\Gamma_{s_j}(T)}{H(T)}. \tag{7}$$

It reaches a maximum at some temperature, $T_{\rm max}$ [49]. If $f_{s_j}(T_{\rm max}) \geq 1$, the sterile state will reach a thermal abundance at early times. We can estimate the contribution to $N_{\rm eff}$ as

$$N_{\rm eff} \simeq N_{\rm eff}^{\rm SM} + \sum_j (1 - \exp(-\alpha f_{s_j}(T^j_{\rm max}))), \tag{8}$$

at decoupling if they are still relativistic, where α is an $\mathcal{O}(1)$ numerical constant. Provided $f_{s_j}(T^j_{\rm max})$ is sufficiently larger than one, $N_{\rm eff}$ saturates to the number of thermalized species, up to exponentially small corrections.

In [43], this result was also derived from the Boltzmann equations [51–54], in the assumption of no primordial large lepton asymmetries. As shown in Appendix A, in spite of the complex 6×6 mixing, the thermalization of the sterile state j is roughly given by the sum of three 2×2 mixing contributions in agreement with the naive expectation of Eq. (6),

$$f_{s_j}(T) = \sum_{\alpha=e,\mu,\tau} \frac{\Gamma_{\nu_\alpha}(T)}{H(T)}\left(\frac{M_j^2}{2pV_\alpha(T) - M_j^2}\right)^2 |(U_{as})_{\alpha j}|^2, \tag{9}$$

where p is the momentum, $V_\alpha(T)$ is the potential induced by coherent scattering in the plasma [50] and $\Gamma_{\nu_\alpha}(T)$ is the scattering rate of the active neutrinos. Both V_α and Γ_α depend on the temperature since the number of scatters increases with T [10,55,56]. While the former varies only when the lepton states become populated, the latter depends significantly on the quark degrees of freedom and therefore changes significantly at the QCD phase transition. The quark contribution to Γ_{ν_α} is however rather uncertain; we therefore neglect this contribution, since this is a conservative assumption if we want to minimize thermalization: any contribution that will increase Γ_{ν_α} would help increase the thermalization rate.

The most complete calculation of Γ_{ν_α} has been presented in [56], where a full two-loop computation of the imaginary part of the neutrino self-energy was presented. The results for the leptonic contribution to $\Gamma_{\nu_\alpha}(T)$ can be accurately parametrized in terms of $C_\alpha(T)$ as

$$\Gamma_{\nu_\alpha} \simeq C_\alpha(T) G_F^2 T^4 p \tag{10}$$

that can be extracted from the numerical results of [56], recently made publicly available in Ref. [57].

For temperatures above the different lepton thresholds, the results can be approximated by
(τ) $T \gtrsim 180$ MeV: $C_{e,\mu,\tau} \simeq 3.43$ and $V_\alpha = AT^4 p$ for $\alpha = e,\mu,\tau$;
(μ) 20 MeV $\lesssim T \lesssim 180$ MeV: $C_{e,\mu} \simeq 2.65$, $C_\tau \simeq 1.26$, $V_e = V_\mu = AT^4 p$ and $V_\tau = BT^4 p$;
(e) $T \lesssim 20$ MeV: $C_e \simeq 1.72$, $C_{\mu,\tau} \simeq 0.95$, $V_e = AT^4 p$ and $V_\mu = V_\tau = BT^4 p$,
with

$$\begin{aligned} B &\equiv -2\sqrt{2}\left(\frac{7\zeta(4)}{\pi^2}\right)\frac{G_F}{M_Z^2}, \\ A &\equiv B - 4\sqrt{2}\left(\frac{7\zeta(4)}{\pi^2}\right)\frac{G_F}{M_W^2}. \end{aligned} \tag{11}$$

In Fig. 1 we show $C_\alpha(T)/\sqrt{g_*(T)}$ as a function of the temperature. We include the T dependent normalization

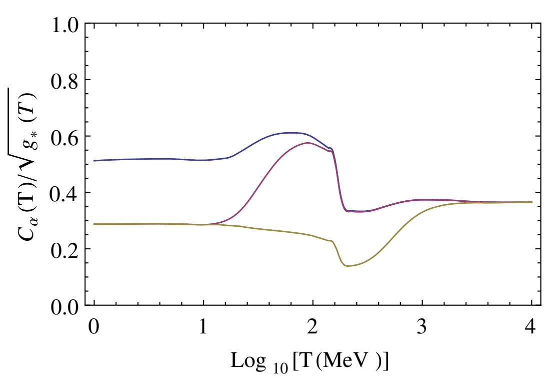

FIG. 1 (color online). Leptonic contribution to $C_\alpha(T)/\sqrt{g_*(T)}$ taken from Refs. [56,57] for $\alpha = e$ (top/blue), μ (middle/magenta), τ (bottom/yellow).

factor, $\sqrt{g_*(T)}$, coming from $H(T)$. Note that the dependence on the temperature of this factor is small.

Let $T_{\max}$ be the value of the temperature at which $f_{s_j}(T)$ is maximum [58]. For $p = 3.15T$, and neglecting the T dependence of $C_\alpha/\sqrt{g_*}$, $T_{\max}$ is bounded by

$$T^\tau_{\max} \equiv \left(\frac{M_j^2}{59.5|A|}\right)^{1/6} \leq T_{\max} \leq \left(\frac{M_j^2}{59.5|B|}\right)^{1/6}. \tag{12}$$

Thermalization will take place provided $f_{s_j}(T_{\max}) \geq 1$. In the next section we derive an analytical lower bound on this quantity, which can be translated therefore into a sufficient condition for thermalization.

III. ANALYTICAL BOUNDS

For a given set of mixing and mass parameters we have the following general lower bound for $f_{s_j}(T)$:

$$f_{\mathrm{B}}(T) \equiv \mathrm{Min}\left[\frac{C_\tau(T)}{\sqrt{g_*(T)}}\right] \frac{G_F^2 p T^4 \sqrt{g_*(T)}}{H(T)} \left(\frac{M_j^2}{2pV_e - M_j^2}\right)^2 \times \sum_{\alpha=e,\mu,\tau} |(U_{as})_{\alpha j}|^2 \leq f_{s_j}(T). \tag{13}$$

This results from the fact that $|V_e| \geq |V_\alpha|$ and $C_\alpha \geq C_\tau$ for all $\alpha = e, \mu, \tau$. The minimization of $C_\tau/\sqrt{g_*}$ as a function of T gets rid of the T dependence of this factor.

The function $f_{\mathrm{B}}(T)$ is maximized at $T^\tau_{\max}$, defined in Eq. (12). It then follows that

$$f_{\mathrm{B}}(T^\tau_{\max}) \leq f_{s_j}(T^\tau_{\max}) \leq f_{s_j}(T_{\max}). \tag{14}$$

In summary, taking the average momentum, $p = 3.15T$, $f_{s_j}(T_{\max})$ is bounded by

$$f_{s_j}(T_{\max}) \geq f_{\mathrm{B}}(T^\tau_{\max}) = \frac{\sum_\alpha |(U_{as})_{\alpha j}|^2 M_j}{3.25 \times 10^{-3}\ \mathrm{eV}}. \tag{15}$$

Using Eq. (4) in the Casas-Ibarra limit, the dependence on the parameters of the model in the above equation can be simplified to the following combination:

$$\sum_\alpha |(U_{as})_{\alpha j}|^2 M_j = \sum_\alpha (U_{\mathrm{PMNS}} m_l^{1/2} R)_{\alpha j} (R^\dagger m_l^{1/2} U^\dagger_{\mathrm{PMNS}})_{j\alpha} = (R^\dagger m_l R)_{jj} \equiv h_j. \tag{16}$$

Therefore the analytical lower bound does not depend on the angles and CP phases of the Pontecorvo-Maki-Nakagawa-Sakata (PMNS) matrix. It depends only on the undetermined Casas-Ibarra parameters and the light neutrino masses. The lower bound can be further simplified using

$$h_j = \sum_\alpha |R_{\alpha j}|^2 m_\alpha \geq |\sum_\alpha R^2_{\alpha j} m_\alpha| \geq |\sum_\alpha R^2_{\alpha j} m_1| = m_1, \tag{17}$$

where in the last step we have used the orthogonality of the R matrix and assumed a normal hierarchy of the light neutrinos (NH). The result for an inverted hierarchy (IH) is the same substituting $m_1 \to m_3$. Finally using Eqs. (16) and (17) in Eq. (15) we obtain

$$f_{s_j}(T_{\max}) \geq \frac{h_j}{3.25 \times 10^{-3}\ \mathrm{eV}} \geq \frac{m_1}{3.25 \times 10^{-3}\ \mathrm{eV}} \equiv \frac{m_1}{m_1^{\mathrm{th}}}, \tag{18}$$

which defines m_1^{th}.

IV. LIGHTEST NEUTRINO MASS VERSUS THERMALIZATION

The thermalization of jth heavy sterile state will occur provided $f_{s_j}(T) \geq 1$ for some T. Therefore a sufficient condition is that $f_{s_j}(T_{\max}) \geq 1$ or using Eq. (18) $m_1 \geq m_1^{\mathrm{th}}$. From the analytical bound we therefore deduce that thermalization of the three states will occur if

$$m_1 \geq 3.25 \times 10^{-3}\ \mathrm{eV}, \tag{19}$$

for any value of the unconstrained parameters in R and the CP phases. We note that a more restrictive upper bound on the lightest neutrino mass was derived in [11,56] under the assumption that M_1 was a warm dark matter candidate in the keV range.

In Fig. 2 we show the contour plots of the minimum of $f_{s_1}(T_{\max})$ (varying the unconstrained parameters in R and the CP phases in the full range), as a function of m_1 and M_1. The three lines correspond to $\mathrm{Min}[f_{s_1}(T_{\max})] = 10^{-1}, 1, 10$. As expected the minimum is strongly correlated with m_1 and is roughly independent of M_1. Values of m_1 below the contour line at 1 correspond to nonthermalization; therefore we read

$$m_1 \leq \mathcal{O}(10^{-3}\ \mathrm{eV}), \tag{20}$$

for $M_1 \in [1\ \mathrm{eV}–100\ \mathrm{MeV}]$. The numerical bound is slightly stronger than the analytical bound given by

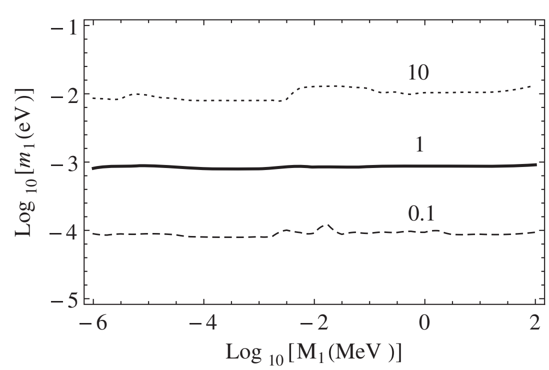

FIG. 2. Contours of $\mathrm{Min}[f_{s_1}(T_{\max})] = 0.1, 1, 10$ on the plane (M_1, m_1).

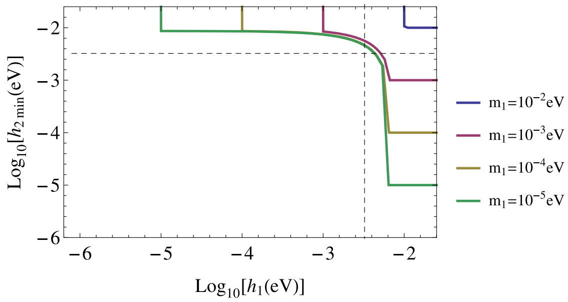

FIG. 3 (color online). Minimum of h_2 in bins of h_1 in the full allowed parameter space with fixed $m_1 = 10^{-[5-2]}$ eV. The dashed line corresponds to the analytical bound $m_1^{\rm th} = 3.25 \times 10^{-3}$ eV.

Eq. (19). Had we considered any other of the heavy states $j = 2, 3$ the results would be the same [i.e. the same minimum of $f_{s_j}(T_{\rm max})$ would be obtained for different values of the unconstrained parameters].

A less stringent (sufficient) condition for thermalization of the state j is

$$h_j \geq m_1^{\rm th} \tag{21}$$

as it follows from Eq. (18). It turns out that this condition is always satisfied for at least two of the three heavy neutrinos, independently of m_1 or the Casas-Ibarra parameters. In Fig. 3 we show the minimization of h_2 in the full parameter space within each bin of h_1, shown in the x-axis, for fixed values of m_1. Although either h_1 or h_2 can always be below the $m_1^{\rm th}$ line (shown as dashed line) if $m_1 \leq m_1^{\rm th}$, the other one is always significantly above it. The same pattern is observed with any pair of h_j. This shows that at most one of the sterile states might not thermalize, and to have one not thermal requires that $m_1 \leq m_1^{\rm th}$.

It is easy to see how h_j can reach its lower bound, m_1, without contradicting present neutrino data. One can always choose $R_{\alpha j} = 0$ for $\alpha \neq j$. For $j = 1$, the orthogonal matrix reduces to the form

$$R = \begin{pmatrix} 1 & 0 \\ 0 & R_{2\times 2} \end{pmatrix}, \tag{22}$$

where $R_{2\times 2}$ is an orthogonal two-dimensional matrix that depends on one complex angle. For $j = 2, 3$ the matrix is analogous with the appropriate permutation of the heavy states. The model therefore reduces in this limit to a $3 + 2 + 1$, where one sterile state is essentially decoupled. When $m_1 \leq m_1^{\rm th}$, the latter might thermalize or not depending on the unknown parameters, while the other two states always thermalize, as in the minimal $3 + 2$ model already considered in Ref. [43].

In the next section we evaluate the implications for $N_{\rm eff}$ in both cases.

V. $N_{\rm EFF}$ IN THE 3 + 3 MODEL

A. $m_1 \geq m_1^{\rm th}$

In this case, the three sterile states thermalize, each of them contributing with $\Delta N_{\rm eff}^{(j)}(T_{d_j}) \approx 1$ at their decoupling temperature, T_{d_j} (provided they are still relativistic). This contribution gets diluted later on, due to the change of $g_*(T)$ between T_{d_j} and the active neutrino decoupling, $T_{\rm BBN}$, when BBN starts. The dilution factor is relevant only for masses larger than $M_j \gtrsim 1$ keV [43].

If they are still relativistic at T_W, we can therefore estimate

$$\Delta N_{\rm eff}^{\rm BBN} = \sum_j \left(\frac{g_*(T_{\rm BBN})}{g_*(T_{d_j})} \right)^{4/3}, \tag{23}$$

where the sum runs over the three heavier states.

For $M_j \geq \mathcal{O}(100)$ MeV, the contribution to the energy density could be significantly suppressed with respect to the estimate Eq. (23), because either they decay sufficiently early before BBN and/or become nonrelativistic at T_{d_j} and therefore get Boltzmann suppressed. Additional constraints will be at work in some regions of parameter space even for those larger masses, but they are likely to depend on the unknown mixing parameters, so we concentrate on the case where at least one of the three heavy neutrinos has a mass below this limit.

We consider in turn the following possibilities.

(i) For all j, $M_j \lesssim 100$ MeV

After recent measurements, the BBN constraints mentioned in the introduction give $\Delta N_{\rm eff}^{\rm BBN} \leq 0.9$ at 2σ. From the results of [43] in the $3 + 2$ model, we estimate that $M_j \lesssim$ 10–100 keV would be excluded from BBN bounds in this case. For larger masses, dilution is sufficiently strong to avoid BBN bounds, but the contribution to the energy density after BBN is anyway too large. When they become nonrelativistic, their contribution to the energy density can be estimated to be [59]

$$\Omega_{s_j} h^2 = 10^{-2} M_j({\rm eV}) \Delta N_{\rm eff}^{(j){\rm BBN}}, \tag{24}$$

where $\Delta N_{\rm eff}^{(j){\rm BBN}}$ is estimated from the ratio of number densities of the jth state and one standard neutrino at BBN. If they do not decay before recombination, Planck constraint on $\Omega_m h^2$ would completely exclude such high masses. On the other hand, if they decay, they transfer this energy density to radiation. The case in which they decay at BBN or before (only for masses above 10 MeV or so) has been considered in detail in [60,61] and essentially BBN constraints, combined with direct search constraints [18,19,62], exclude the range 10–140 MeV. If they decay after BBN, they transfer the energy density mostly to the already decoupled light neutrinos, a contribution that can be parametrized in terms of $\Delta N_{\rm eff}$ which is enhanced with

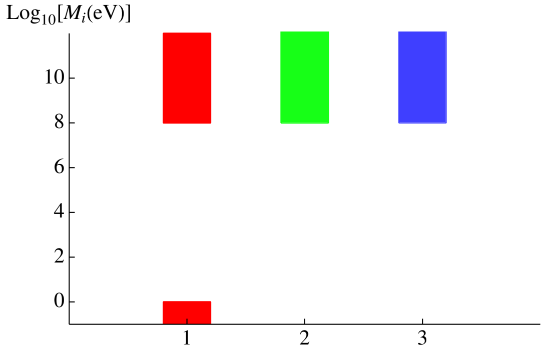

FIG. 4 (color online). Allowed spectra of the heavy states M_i for $m_1 \geq m_1^{\mathrm{th}}$.

respect to that at BBN, Eq. (23), by a factor $\propto \frac{M_j}{T_{\mathrm{dec}}^{(j)}}$, where $T_{\mathrm{dec}}^{(j)}$ is the decay temperature of the jth species. This temperature can be estimated by the relation $H(T_{\mathrm{dec}}^{(j)}) = \tau_{s_j}^{-1}$, where

$$\tau_{s_j}^{-1} \simeq \frac{G_F^2 M_j^5}{192\pi^3} \sum_\alpha |(U_{as})_{\alpha j}|^2 \tag{25}$$

(for M_j below any lepton or hadron threshold). We are not aware of a self-consistent global cosmological analysis of such a scenario. Assuming that CMB constraints on extra radiation ΔN_{eff} roughly apply to it, the large mass region, still allowed by BBN due to dilution, is anyway excluded by CMB measurements, because the ratio $M_j/T_{\mathrm{dec}}^{(j)}$ is very large. Recent analyses on dark radiation from decays can be found in [63–65].

(i) $M_1, M_2 \lesssim 100$ MeV $\ll M_3$

In this case, the results of the $3+2$ model apply directly and the conclusion is the same as before: BBN constraints force the masses to be large to enhance dilution, but such heavy states contribute too much energy density either in the form of matter or extra radiation.

(i) $M_1 \lesssim 100$ MeV $\ll M_2, M_3$

In this case, any value of M_1 could be barely compatible with BBN constraints, since $\Delta N_{\mathrm{eff}} \leq 1$. CMB constraints would however force the state to be very light, sub-eV, which implies $\Delta N_{\mathrm{eff}} \simeq 1$ and therefore some tension with BBN. On the other hand, constraints from oscillations are important in this range [4].

The allowed ranges of the M_j are qualitatively depicted in Fig. 4.

B. $m_1 \leq m_1^{\mathrm{th}}$

If the lightest neutrino mass is below m_1^{th}, one of the states might not thermalize [66], we will take it to be the lightest sterile state although it could be any other. As shown above, this can happen in a region of parameter space with effective decoupling of the first state. A more precise estimate of $\Delta N_{\mathrm{eff}}^{\mathrm{BBN}}$ is given from solving the Boltzmann equations reviewed in Appendix A. We consider two cases:

(i) The unknown mixing parameters (i.e. the Casas-Ibarra parameter of the matrix R and the CP phases) are fixed by minimizing $f_{s_1}(T_{\max})$ and $f_{s_2}(T_{\max})$ as a function of m_1 and M_1, and for fixed values of M_2 and M_3.

(ii) The unknown parameters correspond to those that satisfy $f_{s_1}(T_{\max}) = 10\mathrm{Min}[f_{s_1}(T_{\max})]$ (i.e. the lightest sterile state does not thermalize, but the thermalization rate is ten times larger than its minimum) and minimize $f_{s_2}(T_{\max})$.

In Fig. 5 we show the contribution $\sum_{j=2,3} \Delta N_{\mathrm{eff}}^{(j)\mathrm{BBN}}$ for the NH (IH) cases. It is approximately the same as that found in the $3+2$ model [67] and independent of m_1 and M_1. On the other hand, the contribution $\Delta N_{\mathrm{eff}}^{(1)\mathrm{BBN}}$ depends strongly on m_1 and it is roughly ten times larger in the second case than in the first, as expected from Fig. 2. Assuming that the contribution of the nonthermal state is negligible, the model is still strongly disfavored if $M_2, M_3 \lesssim 100$ MeV, as explained above. The case with $M_2 \lesssim 100$ MeV $\ll M_3$ could be barely compatible with BBN and CMB constraints if $M_2 \lesssim$ eV. The allowed ranges of the M_j are qualitatively depicted in Fig. 6.

When M_2, M_3 are above 100 MeV, the only contribution to ΔN_{eff} would be that of the lighter state. In Fig. 7 we show the contour levels for $\Delta N_{\mathrm{eff}}^{(1)\mathrm{BBN}}$ as obtained from the Boltzmann equations from the ratio of energy (number) densities of the $j=1$ sterile state and one standard neutrino at BBN [see Eqs. (A18) and (A19) in the appendix], versus m_1 and M_1, assuming no lepton asymmetries. In the case of degenerate heavier states significant lepton asymmetries

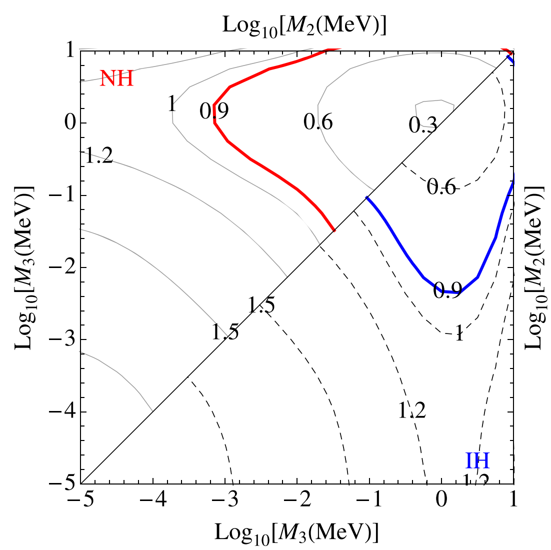

FIG. 5 (color online). $\sum_{j=2,3} \Delta N_{\mathrm{eff}}^{(j)\mathrm{BBN}}$ for $m_1 \leq m_1^{\mathrm{th}}$, as a function of M_2 and M_3. The thick lines correspond to present BBN bounds.

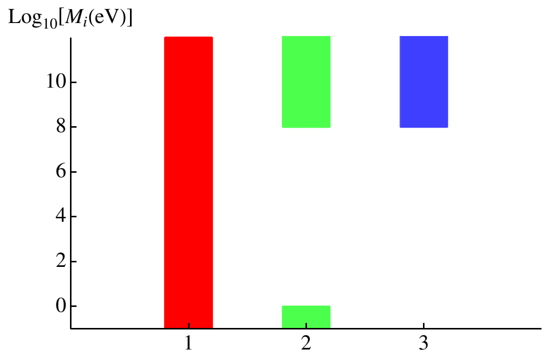

FIG. 6 (color online). Allowed spectra of the heavy states M_i for $m_1 \leq m_1^{\rm th}$. The unconstrained mass could be any $i = 1, 2, 3$.

can be produced [68], which can modify significantly the production of the lighter state [68–70]. We will explore systematically that region of parameter space in a future work, but here we consider only the nondegenerate case where asymmetries are not expected to be of relevance.

In the figure we also included the line, enclosing the shaded region, corresponding to $\Omega_{s_1} h^2 = \Omega_m h^2 = 0.1199$, which is the result from the PLANCK collaboration in a ΛCDM model [24]. In the shaded region the sterile state contributes too much to the matter density and therefore is excluded. Further constraints from Lyman-α and x rays can be found in the recent review [16], and based on the Pauli

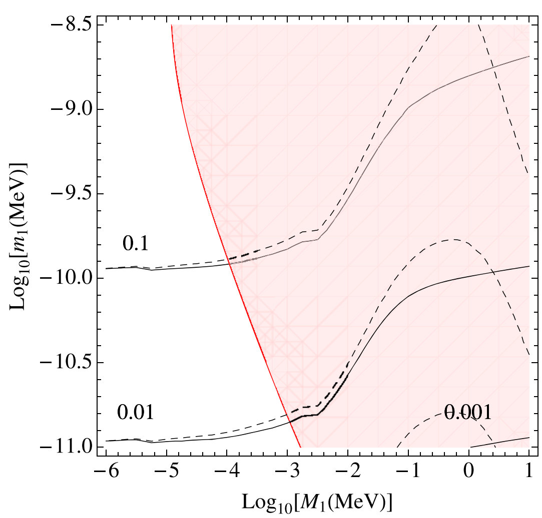

FIG. 7 (color online). Contour plots for $\Delta N_{\rm eff}^{(1){\rm BBN}} = 10^{-1}, 10^{-2}, 10^{-3}$ defined by the ratio of the energy density of the $j = 1$ sterile state and one standard neutrino as a function of m_1 and M_1. The solid (dashed) lines correspond to the contours of the ratio of sterile to active number (energy) densities. The shaded region corresponds to $\Omega_{s_1} h^2 \geq 0.1199$ and the dashed straight line is roughly the one corresponding to decay at recombination. The heavier neutrino masses have been fixed to $M_{2,3} = 1$ GeV, 10 GeV and the unconstrained parameters have been chosen to minimize $f_1(T_{\rm max})$ and $f_2(T_{\rm max})$. The light neutrino spectrum has been assumed to be normal (NH).

exclusion principle and Liouville's theorem in [71]. The almost vertical dashed line corresponds to decay roughly at recombination, which means that in the region to the right of this curve, the $j = 1$ state decays before, and contributes as extra radiation, roughly $\Delta N_{\rm eff}^{(1){\rm BBN}} \times \frac{M_1}{T_{\rm dec}^{(1)}}$, which is much larger than one in the whole plane and is therefore excluded.

We note that for M_1 in the keV range, where it could be a warm dark matter candidate, the allowed region requires $m_1 \lesssim \mathcal{O}(10^{-5}$ eV), which is in good agreement with the bound derived in [15].

We have also studied the case where it is the $j = 2$ state that does not reach thermalization, with $M_1 = 0.5$ eV, $M_3 = 1$ GeV. The contribution of the $j = 2$ state, $\Delta N_{\rm eff}^{(2)}$ is essentially the same as that shown in Fig. 7. In this case the contribution of the lighter state is $\Delta N_{\rm eff}^{(1){\rm BBN}} \simeq 1$, because dilution is very small for such light masses.

All the results we have shown are for a normal hierarchy of the light neutrino spectrum, but the results for IH are almost identical if we exchange $m_1 \to m_3$.

VI. IMPACT ON NEUTRINOLESS DOUBLE BETA DECAY

In the 3 + 3 seesaw models studied here the light and heavy neutrinos are Majorana particles and, therefore, they can contribute to lepton number violating processes such as the neutrinoless double beta ($\beta\beta 0\nu$) decay. The spectra of Fig. 6, allowed if $m_1 \leq m_1^{\rm th}$, will have important implications for this observable for two reasons: (1) the contribution of the light neutrinos to the amplitude of this process, $m_{\beta\beta}$, depends strongly on the lightest neutrino mass and (2) sterile states with masses below 100 MeV could also contribute significantly to this amplitude. The contribution of states with masses well above 100 MeV would be generically subleading [72,73].

If the three heavy states are well above 100 MeV, $m_{\beta\beta}$ is the standard result for the three light Majorana neutrinos. It is shown by the well-known colored bands on Fig. 8 as a function of the lightest neutrino mass, for the two neutrino hierarchies. If one of the states, for example $j = 1$, is in the range [1 eV, 100 MeV], we have seen that it cannot have the thermal abundance which requires an upper bound on the lightest neutrino, $m_1 \leq 10^{-3}$ eV, shown by the vertical dashed grey line. In this case, the sterile state can give a relevant contribution to the amplitude of the process and $m_{\beta\beta}$ reads

$$m_{\beta\beta} = e^{i\alpha} m_1 c_{12}^2 c_{13}^2 + e^{i\beta} m_2 c_{13}^2 s_{12}^2 + m_3 s_{13}^2 + (U_{as})_{e4}^2 M_1. \tag{26}$$

The maximum value of the extra term (with the constraints that the corresponding sterile state does not thermalize, i.e. $f_{s_1}(T_{\rm max}) \leq 1$, and it does not contribute too much to the

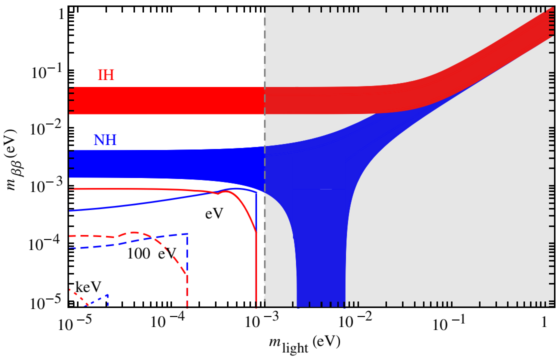

FIG. 8 (color online). $m_{\beta\beta}$ as a function of the lightest neutrino mass: contribution from the active neutrinos (red and blue regions) and the maximum contribution of the lightest sterile neutrino, for $M_1 = 1$ eV (solid), 100 eV (dashed), 1 keV (dotted), for NH (blue) and IH (red) restricting $\Omega_{s_1} h^2 \leq 0.12$ and $f_{s_1}(T_{\rm max}) \leq 1$, for $M_{2,3} \gg 100$ MeV, as a function of the lightest neutrino mass. The shaded region is ruled out for $M_1 \in [1\ \text{eV–}100\ \text{MeV}]$ by the thermalization bound on the lightest neutrino mass, $m_1 \leq 10^{-3}$ eV.

energy density, $\Omega_{s_1} h^2 \leq 0.12$) is shown by the lines for $M_1 = 1$ eV, 100 eV and 1 keV, as a function of the lightest neutrino mass, $m_{\rm light} = m_1(m_3)$ for NH (IH).

Figure 8 shows that the quasidegenerate light neutrino spectrum is ruled out for $M_1 \in [1\ \text{eV–}100\ \text{MeV}]$ and $M_{2,3} \gg 100$ MeV. The region of the parameter space in which a cancellation can occur in the active neutrino contribution is also excluded. It is remarkable that the thermalization bound on $m_{\rm light}$ is around two orders of magnitude stronger than the present constraint on the absolute neutrino mass scale from Planck [24]. On the other hand, we can also conclude that the contribution of the lightest sterile neutrino to the process is subleading and well below the (optimistic) sensitivity of the next-to-next generation of $\beta\beta0\nu$ decay experiments, 10^{-2} eV. This is so, independently of the light neutrino hierarchy.

Finally, there is a still plausible possibility of having a significant contribution to the $\beta\beta0\nu$ decay from a sub-eV thermal sterile neutrino which can satisfy the cosmological bounds. For example, if $f_{s_1}(T_{\rm max}) \geq 1$ with $M_1 \lesssim 1$ eV and $M_{2,3} \gg 100$ MeV, the lightest sterile neutrino could give a significant contribution to the process. However, for such a low M_1 scale, the constraints from neutrino oscillations are expected to be very relevant. Therefore, this case deserves a more careful analysis which should also face the possibility of explaining the neutrino anomalies. This would also apply to the scenario where $M_1 \leq 1$ eV, $1\ \text{eV} \leq M_2 \leq 100$ MeV and $M_3 \gg 100$ MeV, if $m_1 \leq m_1^{\rm th}$. The two lighter states would contribute to $\beta\beta0\nu$. The contribution of M_2 would be similar to that of M_1 in Fig. 8, while that of M_1 would depend significantly on oscillation constraints.

VII. CONCLUSIONS

We have studied the thermalization of the heavy sterile neutrinos in the standard type I seesaw model with three extra singlets and a low scale, $\text{eV} \leq M_j \leq 100$ MeV. The production of the states in the early Universe occurs via nonresonant mixing (in the absence of large primordial asymmetries) and we have found that, independently of the unknown mixing parameters in the model, full thermalization is always reached for the three states if the lightest neutrino mass is above $\mathcal{O}(10^{-3}\ \text{eV})$. Since they decouple early, while they are still relativistic, these states either violate BBN constraints on $\Delta N_{\rm eff}$ and/or contribute too much energy density to the Universe at later times, either in the form of cold dark matter (if they decay late enough) or in the form of dark radiation (if they decay earlier). Majorana masses would all need to be heavier than $\mathcal{O}(100\ \text{MeV})$ to avoid cosmology constraints, or alternatively one of them could remain very light sub-eV, resulting in a milder tension with cosmology.

In contrast, if the lightest neutrino mass is below $\mathcal{O}(10^{-3}\ \text{eV})$, one and only one of the sterile states might never thermalize, depending on the unknown parameters of the model, and therefore its mass is unconstrained. The other two states always thermalize and therefore their masses should be above $\mathcal{O}(100\ \text{MeV})$ to avoid cosmological constraints. The scenario often referred to as the νMSM [15] falls in this category, where the nonthermalized state in the keV region could be a candidate for warm dark matter [8,11] and the heavier states could generate the baryon asymmetry [14]. In fact, a more stringent upper bound on m_1 had been previously derived from the requirement that $M_1 \sim$ keV and could be a warm dark matter candidate [15]. Alternatively, the tension with cosmology could also be minimized in this case if one of the two thermalized states is very light sub-eV and the other remains heavy.

Although the possibility of having one of the species in the sub-eV range could provide an interesting scenario to maybe explain the neutrino oscillation anomalies, the tension between cosmology and neutrino oscillation experiments is likely to be significant.

Finally, we have also studied the impact of the cosmological bounds extracted in this work on the $\beta\beta0\nu$ decay phenomenology. We have found that if one of the sterile neutrinos does not thermalize, the quasidegenerate light neutrino spectrum would be ruled out. The region of the parameter space in which a cancellation can take place in the active neutrino contribution is also excluded in this scenario. In addition, we have also shown that the contributions of sterile states with $M_1 \in [1\ \text{eV–}100\ \text{MeV}]$ are subleading and well beyond the sensitivity of the next-to-next generation of $\beta\beta0\nu$ decay experiments. However, a sub-eV thermal sterile state could give a contribution, in this scenario, within reach of the next-to-next generation of

$\beta\beta 0\nu$ decay experiments, the constraints from neutrino oscillations playing a very important role.

ACKNOWLEDGMENTS

We thank M. Laine for providing us with data files with the numerical results of Ref. [56] in an easy-to-use format. We also thank A. Donini, E. Fernández-Martínez, O. Mena, S. Petcov and A.Vincent for useful discussions. This work was partially supported by Grants FPA2011-29678, PROMETEO/2009/116, CUP (CSD2008-00037), ITN INVISIBLES (Marie Curie Actions, PITN-GA-2011-289442) and the INFN program on "Astroparticle Physics." J. López-Pavón acknowledges NORDITA for the hospitality during the "News in Neutrino Physics" workshop, where part of this work was done. M. Kekic thanks the IFT-UAM/CSIC institute for hospitality while this work was done.

APPENDIX:

In the density matrix formalism [54], the kinetic equations have the usual form:

$$\dot{\rho} = -i[H,\rho] - \frac{1}{2}\{\Gamma, \rho - \rho_{\rm eq} I_A\}, \tag{A1}$$

where ρ is the 6×6 density matrix, H is the Hamiltonian describing the propagation of relativistic neutrinos in the plasma, Γ is the collision term that we take from Refs. [56,57] and $\rho_{\rm eq}$ is the active neutrino thermal density, i.e. the Fermi-Dirac distribution $\rho_{\rm eq} = \frac{1}{e^{E/T}+1}$, in the absence of a chemical potential. I_A is the projector on the active sector. The trace of the density matrix corresponds to the number density of neutrinos.

Rewriting Eq. (A1) in the form of active-sterile block matrices we get the following set of equations:

$$\dot{\rho}_A = -i(H_A\rho_A - \rho_A H_A + H_{AS}\rho_{AS}^\dagger - \rho_{AS}H_{AS}^\dagger) - \frac{1}{2}\{\Gamma_A, \rho_A - \rho_{\rm eq} I_A\}, \tag{A2}$$

$$\dot{\rho}_{AS} = -i(H_A\rho_{AS} - \rho_A H_{AS} + H_{AS}\rho_S - \rho_{AS}H_S) - \frac{1}{2}\Gamma_A\rho_{AS}, \tag{A3}$$

$$\dot{\rho}_S = -i(H_{AS}^\dagger\rho_{AS} - \rho_{AS}^\dagger H_{AS} + H_S\rho_S - \rho_S H_S). \tag{A4}$$

Assuming that $\Gamma_A \gg$ Hubble rate, we can approximate

$$\dot{\rho}_A = \dot{\rho}_{AS} = 0. \tag{A5}$$

This is the so-called "static approximation" [33,69,70].

The first equation implies $\rho_A = \rho_{\rm eq} I_A$, while the second equality implies

$$(\rho_{AS})_{ai} = (-(H_A - \tilde{H}_i I_A) + i\Gamma_A/2)^{-1}_{aa'}(H_{AS})_{a'j}((\rho_S)_{ji} - \rho_{\rm eq}\delta_{ji}), \tag{A6}$$

where we have made the approximation that $(H_S)_{ij} = \tilde{H}_i\delta_{ij}$, which is very good in the seesaw limit. Similarly we find

$$(\rho_{AS}^\dagger)_{ia} = ((\rho_S)_{ij} - \rho_{\rm eq}\delta_{ij})(H_{AS}^\dagger)_{ja'}(-(H_A - \tilde{H}_i I_A) - i\Gamma_A/2)^{-1}_{a'a}. \tag{A7}$$

Defining $\tilde{\rho}_S \equiv \rho_S - \rho_{\rm eq} I_S$, and after substituting ρ_{AS} and $\rho_{AS}^\dagger$ in Eq. (A4), we get the following equation:

$$\begin{aligned}(\dot{\rho}_S)_{ij} = {}& -i(\tilde{H}_i - \tilde{H}_j)(\rho_S)_{ij} \\ & - i(H_{AS}^\dagger)_{a'i}(-(H_A - \tilde{H}_j I_A) \\ & + i\Gamma_A/2)^{-1}_{a'a}(H_{AS})_{ak}\tilde{\rho}_{kj} \\ & + i\tilde{\rho}_{ik}(H_{AS}^\dagger)_{a'k}(-(H_A - \tilde{H}_i I_A) \\ & - i\Gamma_A/2)^{-1}_{a'a}(H_{AS})_{aj}.\end{aligned} \tag{A8}$$

It is clear that the equilibrium distribution for the sterile components is $\tilde{\rho}_{ii} = 0$ or $\rho_{ii} = \rho_{eq}\delta_{ii}$.

At this point it is necessary to solve the 3×3 system of differential equations (A8), but we can further simplify the problem if we assume that the dynamics of the different sterile components decouple from each other, which is the case provided their masses are sufficiently different. Since H_{AS} depends on temperature, if the sterile splittings are significantly different from each other, we will generically have that H_{AS} will be very suppressed unless the temperature-dependent effective mass is similar to one of the mass splittings. Let us suppose that this is the case. At high T all active-sterile mixings are very suppressed, until one splitting that associated to the sterile state s is reached; at this point only $(H_{AS})_{as}$ is non-negligible. Then only $(\rho_S)_{ss}$ changes significantly and can be described by

$$\begin{aligned}\dot{\rho}_{ss} &= -i\left(H_{AS}^\dagger\left\{\frac{1}{-(H_A - \tilde{H}_s) + i\Gamma_A/2} - \frac{1}{-(H_A - \tilde{H}_s) - i\Gamma_A/2}\right\}H_{AS}\right)_{ss}\tilde{\rho}_{ss} \\ &= -\left(H_{AS}^\dagger\left\{\frac{\Gamma_A}{(H_A - \tilde{H}_s)^2 + \Gamma_A^2/4}\right\}H_{AS}\right)_{ss}\tilde{\rho}_{ss},\end{aligned} \tag{A9}$$

where in the last step we have assumed that H_A, Γ_A commute, which again is a good approximation in the seesaw limit. This equation justifies Eq. (6), since the source term on the right of Eq. (A9) is the same as Γ_s in Eq. (6) if we neglect the term $\sim\Gamma_A^2$ in the denominator. We have checked that the result of solving the three coupled equations or the three independent ones gives very similar results and the latter is obviously much faster.

Now we have to consider the evolution in an expanding universe, where the variation of the scale factor $a(t)$ depends on the Hubble expansion rate, which, in a radiation-dominated universe at temperature T, is given by

$$H(T) = \sqrt{\frac{8\pi G_N}{3}\left(\frac{\pi^2}{30}g_*(T)T^4 + \epsilon_s(T)\right)}, \tag{A10}$$

where g_* counts the relativistic degrees of freedom and we have included the contribution to the energy density of the sterile states, ϵ_s, which must be computed integrating the trace of the density matrix, ρ_S. As in Ref. [33] we introduce new variables:

$$x = \frac{a(t)}{a_{\rm BBN}}, \qquad y = x\frac{p}{T_{\rm BBN}}, \tag{A11}$$

where $a(t)$ is the cosmic scale factor, $T_{\rm BBN} \simeq 1$ MeV is the temperature of active neutrino decoupling and $a_{\rm BBN}$ the scale factor at this point. On the other hand, entropy conservation implies $g_{S*}(T)T^3a(t)^3 = \text{constant}$ (here g_{S*} refers to the relativistic degrees of freedom in equilibrium; it differs from g_* in the Hubble expansion only after light neutrino decoupling). This relation implies

$$x = \frac{T_{\rm BBN}}{T}\left(\frac{g_{S*}(T_{\rm BBN})}{g_{S*}(T)}\right)^{1/3}. \tag{A12}$$

We neglect the contribution of the sterile states to g_{S*}, because they decouple very early and therefore they give a small contribution.

The time derivative acting on any phase space distribution can be written as

$$\frac{d}{dt}f(t,p) = (\partial_t - Hp\partial_p)f(t,p) = Hx\partial_x f(x,y). \tag{A13}$$

Applied to Eq. (A1) this leads to

$$Hx\frac{\partial}{\partial x}\rho(x,y)\Big|_y = -i[\hat{H},\rho(x,y)] - \frac{1}{2}\{\Gamma, \rho(x,y) - \rho_{\rm eq}(x,y)I_A\}, \tag{A14}$$

where

$$\rho_{\rm eq}(x,y) = \frac{1}{\exp\left[y(g_{S*}(T(x))/g_{S*}(T_{\rm BBN}))^{1/3}\right]+1}, \tag{A15}$$

and for Eq. (A9) similarly

$$Hx\frac{\partial}{\partial x}\rho_{ss}(x,y)\Big|_y = -\left(H^\dagger_{AS}\left\{\frac{\Gamma_A}{(H_A - \tilde{H}_s)^2 + \Gamma_A^2/4}\right\}H_{AS}\right)_{ss}\tilde{\rho}_{ss}(x,y). \tag{A16}$$

The equations are evolved from an initial condition at $x_i \to 0$, $\rho_{ss} = 0$, until active neutrino decoupling, $x_f = 1$ for fixed y. We define the effective number of additional neutrino species by

$$\Delta N_{\rm eff} = \frac{\epsilon_s}{\epsilon_\nu^0}, \tag{A17}$$

where ϵ_ν^0 is the energy density of one SM massless neutrino. For each additional neutrino we compute the contribution to $\Delta N_{\rm eff}$ from the solution of $\rho_{s_js_j}(x_f,y)$ as

$$\Delta N_{\rm eff}^{(j){\rm BBN}}|_{\rm energy} = \frac{\int {\rm d}yy^2E(y)\rho_{s_js_j}(x_f,y)}{\int {\rm d}yy^2p(y)\rho_{\rm eq}(x_f,y)}, \tag{A18}$$

where $p(y) = \frac{y}{x_f}T_{\rm BBN}$ and $E(y) = \sqrt{p(y)^2 + M_j^2}$.

We can also define the ratio of number densities instead, which is more appropriate when they are not relativistic,

$$\Delta N_{\rm eff}^{(j){\rm BBN}}|_{\rm number} = \frac{\int {\rm d}yy^2\rho_{s_js_j}(x_f,y)}{\int {\rm d}yy^2\rho_{\rm eq}(x_f,y)}. \tag{A19}$$

The two correspond to the solid/dashed curves depicted in Fig. 7.

[1] P. Minkowski, Phys. Lett. **67B**, 421 (1977); M. Gell-Mann, P. Ramond, and R. Slansky, in *Supergravity*, edited by P. van Nieuwenhuizen and D. Freedman (North-Holland, Amsterdam, 1979), p. 315; T. Yanagida in *Proceedings of the Workshop on the Unified Theory and the Baryon Number in the Universe*, edited by O. Sawada and A. Sugamoto (KEK Report No. 79-18, Tsukuba, 1979), p. 95; R. N. Mohapatra and G. Senjanovic, Phys. Rev. Lett. **44**, 912 (1980).

[2] The range 10^{-10}–1eV can be excluded from oscillation data [3,4], while a scale above 10^{15} GeV would require nonperturbative Yukawa couplings.
[3] A. de Gouvea, Phys. Rev. D **72**, 033005 (2005); A. de Gouvea, J. Jenkins, and N. Vasudevan, Phys. Rev. D **75**, 013003 (2007).
[4] A. Donini, P. Hernández, J. López-Pavón, and M. Maltoni, J. High Energy Phys. 07 (2011) 105.
[5] A. Aguilar-Arevalo *et al.* (LSND Collaboration), Phys. Rev. D **64**, 112007 (2001).
[6] A. A. Aguilar-Arevalo *et al.* (MiniBooNE Collaboration), Phys. Rev. Lett. **110**, 161801 (2013).
[7] G. Mention, M. Fechner, Th. Lasserre, Th. A. Mueller, D. Lhuillier, M. Cribier, and A. Letourneau, Phys. Rev. D **83**, 073006 (2011); P. Huber, Phys. Rev. C **84**, 024617 (2011); **85**, 029901 (2012).
[8] S. Dodelson and L. M. Widrow, Phys. Rev. Lett. **72**, 17 (1994).
[9] X.-D. Shi and G. M. Fuller, Phys. Rev. Lett. **82**, 2832 (1999).
[10] K. Abazajian, G. M. Fuller, and M. Patel, Phys. Rev. D **64**, 023501 (2001).
[11] T. Asaka, S. Blanchet, and M. Shaposhnikov, Phys. Lett. B **631**, 151 (2005).
[12] E. Bulbul, M. Markevitch, A. Foster, R. K. Smith, M. Loewenstein, and S. W. Randall, Astrophys. J. **789**, 13 (2014).
[13] A. Boyarsky, O. Ruchayskiy, D. Iakubovskyi, and J. Franse, arXiv:1402.4119.
[14] E. K. Akhmedov, V. A. Rubakov, and A. Y. Smirnov, Phys. Rev. Lett. **81**, 1359 (1998).
[15] T. Asaka and M. Shaposhnikov, Phys. Lett. B **620**, 17 (2005).
[16] L. Canetti, M. Drewes, T. Frossard, and M. Shaposhnikov, Phys. Rev. D **87**, 093006 (2013), and references therein.
[17] S. Antusch, C. Biggio, E. Fernandez-Martinez, M. B. Gavela, and J. Lopez-Pavon, J. High Energy Phys. 10 (2006) 084; A. Abada, C. Biggio, F. Bonnet, M. B. Gavela, and T. Hambye, J. High Energy Phys. 12 (2007) 061; S. Antusch, J. P. Baumann, and E. Fernandez-Martinez, Nucl. Phys. **B810**, 369 (2009); D. N. Dinh, A. Ibarra, E. Molinaro, and S. T. Petcov, J. High Energy Phys. 08 (2012) 125; 09 (2013) 023; R. Alonso, M. Dhen, M. B. Gavela, and T. Hambye, J. High Energy Phys. 01 (2013) 118; D. N. Dinh and S. T. Petcov, J. High Energy Phys. 09 (2013) 086.
[18] D. Gorbunov and M. Shaposhnikov, J. High Energy Phys. 10 (2007) 015.
[19] A. Atre, T. Han, S. Pascoli, and B. Zhang, J. High Energy Phys. 05 (2009) 030.
[20] R. Foot, M. J. Thomson, and R. R. Volkas, Phys. Rev. D **53**, R5349 (1996).
[21] S. Hannestad, R. S. Hansen, and T. Tram, Phys. Rev. Lett. **112**, 031802 (2014).
[22] B. Dasgupta and J. Kopp, Phys. Rev. Lett. **112**, 031803 (2014).
[23] R. Cooke, M. Pettini, R. A. Jorgenson, M. T. Murphy, and C. C. Steidel, arXiv:1308.3240 [Astrophys. J. (to be published)].
[24] P. A. R. Ade *et al.* (Planck Collaboration), Astron. Astrophys., doi:10.1051/0004-6361/201321591, 2014.
[25] G. Hinshaw *et al.* (WMAP Collaboration), Astrophys. J. Suppl. Ser. **208**, 19 (2013).
[26] Z. Hou *et al.*, Astrophys. J. **782**, 74 (2014).
[27] J. L. Sievers *et al.*, J. Cosmol. Astropart. Phys. 10 (2013) 060.
[28] P. A. R. Ade *et al.* (BICEP2 Collaboration), Phys. Rev. Lett. **112**, 241101 (2014).
[29] P. A. R. Ade *et al.* (BICEP2 Collaboration), Astrophys. J. **792**, 62 (2014).
[30] E. Giusarma, E. Di Valentino, M. Lattanzi, A. Melchiorri, and O. Mena, Phys. Rev. D **90**, 043507 (2014).
[31] M. Archidiacono, N. Fornengo, S. Gariazzo, C. Giunti, S. Hannestad, and M. Laveder, J. Cosmol. Astropart. Phys. 06 (2014) 031.
[32] J. Bergström, M. C. Gonzalez-Garcia, V. Niro, and J. Salvado, arXiv:1407.3806.
[33] A. D. Dolgov and F. L. Villante, Nucl. Phys. **B679**, 261 (2004).
[34] M. Cirelli, G. Marandella, A. Strumia, and F. Vissani, Nucl. Phys. **B708**, 215 (2005).
[35] A. Melchiorri, O. Mena, S. Palomares-Ruiz, S. Pascoli, A. Slosar, and M. Sorel, J. Cosmol. Astropart. Phys. 01 (2009) 036.
[36] S. Hannestad, I. Tamborra, and T. Tram, J. Cosmol. Astropart. Phys. 07 (2012) 025.
[37] E. Kuflik, S. D. McDermott, and K. M. Zurek, Phys. Rev. D **86**, 033015 (2012).
[38] A. Mirizzi, N. Saviano, G. Miele, and P. D. Serpico, Phys. Rev. D **86**, 053009 (2012).
[39] T. D. Jacques, L. M. Krauss, and C. Lunardini, Phys. Rev. D **87**, 083515 (2013).
[40] N. Saviano, A. Mirizzi, O. Pisanti, P. Serpico, G. Mangano, and G. Miele, Phys. Rev. D **87**, 073006 (2013).
[41] M. Archidiacono, N. Fornengo, C. Giunti, S. Hannestad, and A. Melchiorri, Phys. Rev. D **87**, 125034 (2013).
[42] A. Mirizzi, G. Mangano, N. Saviano, E. Borriello, C. Giunti, G. Miele, and O. Pisanti, Phys. Lett. B **726**, 8 (2013).
[43] P. Hernandez, M. Kekic, and J. Lopez-Pavon, Phys. Rev. D **89**, 073009 (2014).
[44] M. Shaposhnikov, J. High Energy Phys. 08 (2008) 008.
[45] J. A. Casas and A. Ibarra, Nucl. Phys. **B618**, 171 (2001).
[46] A. Donini, P. Hernández, J. López-Pavón, M. Maltoni, and T. Schwetz, J. High Energy Phys. 07 (2012) 161.
[47] M. Blennow and E. Fernandez-Martinez, Phys. Lett. B **704**, 223 (2011).
[48] There is an upper bound for the lightest neutrino mass but no lower bound exists at present.
[49] R. Barbieri and A. Dolgov, Phys. Lett. B **237**, 440 (1990); Nucl. Phys. **B349**, 743 (1991); K. Kainulainen, Phys. Lett. B **244**, 191 (1990).
[50] D. Notzold and G. Raffelt, Nucl. Phys. **B307**, 924 (1988).
[51] L. Stodolsky, Phys. Rev. D **36**, 2273 (1987); G. Raffelt, G. Sigl, and L. Stodolsky, Phys. Rev. Lett. **70**, 2363 (1993); M. J. Thomson, Phys. Rev. A **45**, 2243 (1992).
[52] K. Enqvist, K. Kainulainen, and M. Thomson, Nucl. Phys. **B373**, 498 (1992); B. H. J. McKellar and M. J. Thomson, Phys. Rev. D **49**, 2710 (1994).
[53] G. Sigl and G. Raffelt, Nucl. Phys. **B406**, 423 (1993).

[54] A. D. Dolgov, Phys. Rep. **370**, 333 (2002).
[55] K. N. Abazajian and G. M. Fuller, Phys. Rev. D **66**, 023526 (2002); K. Abazajian, Phys. Rev. D **73**, 063506 (2006).
[56] T. Asaka, M. Laine, and M. Shaposhnikov, J. High Energy Phys. 01 (2007) 091.
[57] Data files for the imaginary part of the neutrino self-energy have been made available in http://www.laine.itp.unibe.ch/neutrino-rate/.
[58] We note that $T_{\max}$ depends on M_j, but to simplify notation we skip the index j in this quantity.
[59] E. W. Kolb and M. S. Turner, Front. Phys. **69**, 1 (1990).
[60] A. D. Dolgov, S. H. Hansen, G. Raffelt, and D. V. Semikoz, Nucl. Phys. **B580**, 331 (2000); , **B590**, 562 (2000).
[61] O. Ruchayskiy and A. Ivashko, J. Cosmol. Astropart. Phys. 10 (2012) 014.
[62] O. Ruchayskiy and A. Ivashko, J. High Energy Phys. 06 (2012) 100.
[63] M. C. Gonzalez-Garcia, V. Niro, and J. Salvado, J. High Energy Phys. 04 (2013) 052.
[64] J. Hasenkamp and J. Kersten, J. Cosmol. Astropart. Phys. 08 (2013) 024.
[65] J. Hasenkamp, arXiv:1405.6736.
[66] There are always ranges of parameters where it does thermalize and in this case the same conclusions apply as in the previous section.
[67] The small differences with respect to the results in [43] are due to the more precise scattering rates Γ_α used here.
[68] M. Laine and M. Shaposhnikov, J. Cosmol. Astropart. Phys. 06 (2008) 031.
[69] R. Foot and R. R. Volkas, Phys. Rev. D **55**, 5147 (1997).
[70] N. F. Bell, R. R. Volkas, and Y. Y. Y. Wong, Phys. Rev. D **59**, 113001 (1999).
[71] A. Boyarsky, O. Ruchayskiy, and D. Iakubovskyi, J. Cosmol. Astropart. Phys. 03 (2009) 005.
[72] M. Blennow, E. Fernandez-Martinez, J. Lopez-Pavon, and J. Menendez, J. High Energy Phys. 07 (2010) 096.
[73] J. Lopez-Pavon, S. Pascoli, and C.-f. Wong, Phys. Rev. D **87**, 093007 (2013).